FEBS Letters 586 (2012) 3705–3709

FEBS Letters
journal homepage: www.FEBSLetters.org

Crystal structure analysis of the translation factor RF3 (release factor 3)

Kiyohito Kihira [a], Yoshihiro Shimizu [b], Yasuhito Shomura [a], Naoki Shibata [a], Masaya Kitamura [c], Atsushi Nakagawa [d], Takuya Ueda [e], Kozo Ochi [f], Yoshiki Higuchi [a,*]

[a] Graduate School of Life Science, University of Hyogo, Ako 678-1297, Japan
[b] Laboratory for Cell-Free Protein Synthesis, RIKEN Quantitative Biology Center, Kobe 650-0047, Japan
[c] Graduate School of Engineering, Osaka City University, Osaka 558-8585, Japan
[d] Institute for Protein Research, Osaka University, Suita 565-0871, Japan
[e] Graduate School of Frontier Sciences, University of Tokyo, Kashiwa 277-8562, Japan
[f] Department of Life Science, Hiroshima Institute of Technology, Hiroshima 731-5193, Japan

ARTICLE INFO

Article history:
Received 9 July 2012
Revised 22 August 2012
Accepted 22 August 2012
Available online 6 September 2012

Edited by Michael Ibba

Keywords:
GTPase
Release factor
Ribosome
Translation
Stringent response

ABSTRACT

The bacterial translational GTPases release factor RF3 promotes translation termination by recycling RF1 or RF2. Here, we present the crystal structures of RF3 complexed with GDP and guanosine 3′,5′-(bis)diphosphate (ppGpp) at resolutions of 1.8 and 3.0 Å, respectively. ppGpp is involved in the so-called "stringent response" of bacteria. ppGpp binds at the same site as GDP, suggesting that GDP and ppGpp are two alternative physiologically relevant ligands of RF3. We also found that ppGpp decelerates the recycling of RF1 by RF3. These lines of evidence suggest that RF3 functions both as a cellular metabolic sensor and as a regulator.

1. Introduction

In response to a stop codon, RF1 and RF2 hydrolyze and release the completed polypeptide from the peptidyl-tRNA. RF3 catalyzes the removal of RF1 or RF2, acting in a GTP-dependent manner [1]. Free RF3 exists almost exclusively in the GDP-bound form. Recently, the X-ray structures of RF3 from *Escherichia coli* (*Ec*RF3) in the GDP-bound form and the ribosome-bound *Ec*RF3•GDPNP form have been reported [2–4]. These reports suggest that the binding of RF3•GTP leads to large conformational changes of the ribosome. However, in the X-ray crystal structure of the RF3•GDP complex, the switch-1 region, which is functionally important and conserved among G proteins [5], was disordered. Therefore, the details of the molecular mechanism for the RF1/RF2 recycling catalyzed by RF3 remain unclear.

In cells growing under optimal conditions, the concentrations of GDP and GTP are much higher than those of bacterial alarmone guanosine 3′,5′-(bis)diphosphate (ppGpp). After multiple types of nutritional stress, however, the concentration of ppGpp increases significantly (i.e., up to 2 mM), becoming more abundant than GDP and bacterial cells exert stringent control [6]. This so-called "stringent response" is one of the most important adaptations by which bacteria survive harsh conditions. In addition, recent studies have demonstrated that ppGpp is present not only in bacteria but also in plants [7]. It is likely that these concentration shifts affect the functions of GTP-binding proteins. However, little is known about the role ppGpp plays as a factor in the stringent response on the ribosomal termination complex.

In this study, we found that RF3 binds ppGpp as well as GDP and GTP, and that ppGpp slows translation by selectively targeting RF3 activities. We also report the crystal structures of RF3 from *Desulfovibrio vulgaris* Miyazaki F (*Dv*RF3) in complex with GDP and ppGpp, establishing a detailed reaction mechanism for the final stage of translation of mRNA.

2. Materials and methods

2.1. Sample preparation and structure determination

Recombinant RF3 was expressed (Supplementary data), purified, and crystallized as previously described [8]. The structure of RF3 in complex with GDP was solved by molecular replacement using the coordinates of *Ec*RF3 (PDB code 2h5e). The structure of RF3 in complex with ppGpp was solved using the coordinates of

* Corresponding author. Address: University of Hyogo, 3-2-1 Koto, Kamigori-cho, Ako-gun, Hyogo 678-1297, Japan. Fax: +81 791 58 0177.
E-mail address: hig@sci.u-hyogo.ac.jp (Y. Higuchi).

0014-5793/$36.00 © 2012 Federation of European Biochemical Societies. Published by Elsevier B.V. All rights reserved.
http://dx.doi.org/10.1016/j.febslet.2012.08.029

*Dv*RF3•GDP. Detailed procedures of the structure determination are described in the Supplementary data.

2.2. RF1 recycling assay

The release complex (RC) was generated using the PURE system [9], which was reconstructed from its highly purified components. In this experiment, the amount of RC was present in considerable excess relative to the release factors, such that the release factors were recycled multiple times until all RC in the assay system were completely consumed by release of nascent peptides from RC [1]. In the reaction mixture, 80 pmol RC, 2 pmol RF1, 20 pmol RF3 and 2 mM guanine nucleotides (GDP and ppGpp) were used for the RF1 recycling experiments. Detailed procedures are described in the Supplementary data.

2.3. Analysis of the nucleotide binding state of DvRF3 under various conditions

Escherichia coli strain BL21 (DE3) cells transformed with plasmids encoding RF3 were grown at 37 °C after exponential phase of growth in M9-casamino acids medium containing isopropyl β-D-1-thiogalactopyranoside at a final concentration of 0.1 mM as well as antibiotics corresponding to the selection markers on the expression vectors. The sample preparation was carried out as described above.

For gel-shift assays, *Dv*RF3 samples were incubated with nucleotides at various concentrations at room temperature for 30 min. Each reaction mixture was subjected to polyacrylamide gel electrophoresis in the native state.

3. Results and discussion

3.1. Purification of DvRF3

*Dv*RF3 was prepared from *E. coli* BL21 (DE3) cells transformed with the plasmid pUTRF3 [8] and harvested after exponential phase of growth. After Ni-affinity chromatography, the protein was separated into two peaks by DEAE chromatography (Fig. S1A). These two *Dv*RF3 components (Peak-1 and Peak-2) showed almost identical patterns of absorption spectra and relative mobility in SDS–PAGE (Fig. S1B), whereas they are distinguishable by native PAGE (Fig. S1C). Peak-1 and Peak-2 were revealed to represent the GDP-bound and ppGpp-bound forms, respectively, as confirmed by gel-shift assay and the X-ray structure analysis described in this study. In the gel-shift assay, Peak-1 without additional nucleotides was at the same position as that with GDP. On the contrary, Peak-2 was at the same position as that with ppGpp (Fig. S1C). The mobility in the gel did not change by the addition of ppApp (an analog of ppGpp).

3.2. Overall structure of DvRF3•GDP and DvRF3•ppGpp

The structure of *Dv*RF3 in complex with GDP (Peak-1) was solved at 1.8 Å resolution (Table S1). The polypeptide chain of *Dv*RF3•GDP is folded into three distinct domains (Fig. 1B and S2). The tertiary structure of *Dv*RF3•GDP is strikingly similar to that of *Ec*RF3•GDP (Fig. 1A) with a root mean square deviation (rmsd) of 1.1 Å. The switch-1 region of *Ec*RF3•GDP is disordered, whereas a part of the corresponding region of *Dv*RF3•GDP forms an α-helical structure, which is not observed in other translational GTPases in complex with GDP (residues 38–47). The interactions of GDP with the amino acid residues of RF3 are very similar to those of *Ec*RF3 (Fig. S3). The structure of *Dv*RF3 (Peak-2) was solved at 3.0 Å resolution (Table S1). The 2*Fo-Fc* electron density map calculated using the model of RF3•GDP revealed that a residual density peak extended from the 3′-end of the GDP, indicating that ppGpp rather than GTP is bound at the GDP-binding site (Fig. 2C). The tertiary structures of *Dv*RF3•ppGpp and *Dv*RF3•GDP are superimposable with an rmsd of 0.65 Å. In the *Dv*RF3•ppGpp structure, the switch-1 region is also well-ordered and contains a longer α helix than that in *Dv*RF3•GDP, which is followed by two short α helices, probably due to the interaction between Nε of Lys49 and the 3′ diphosphate group of ppGpp (Figs. 1B and C and 2B). This diphosphate group protrudes from the molecular surface of *Dv*RF3 (Fig. 2D), suggesting that the switch-1 region of *Dv*RF3•ppGpp is less flexible than in *Dv*RF3•GDP, which is followed by two short α helices, probably due to the interaction between *N*ε of Lys4. The structure of the switch-1 region in *Dv*RF3•ppGpp is quite different from that of ribosome•*Ec*RF3•GDPNP [2] (Fig. 1D).

3.3. Gel shift assay of RF3

In all bacteria which possess a *prfC* gene (encoding RF3), the residue corresponding to Lys49 in *Dv*RF3•GDP is predominantly either lysine or glycine, with lysine more frequently observed (Table S2). In addition, Ala47 in the switch-1 helix also seems to play a role in stabilizing this region: alanine and leucine usually stabilize α-helical structure, whereas proline and glycine tend to destabilize helices [10,11]. Ala47 and Lys49 of *Dv*RF3 correspond to Gly48 and Gly50 of *Ec*RF3, respectively. To clarify the functional roles of these residues, the ppGpp-binding affinity of the variants of K49G and

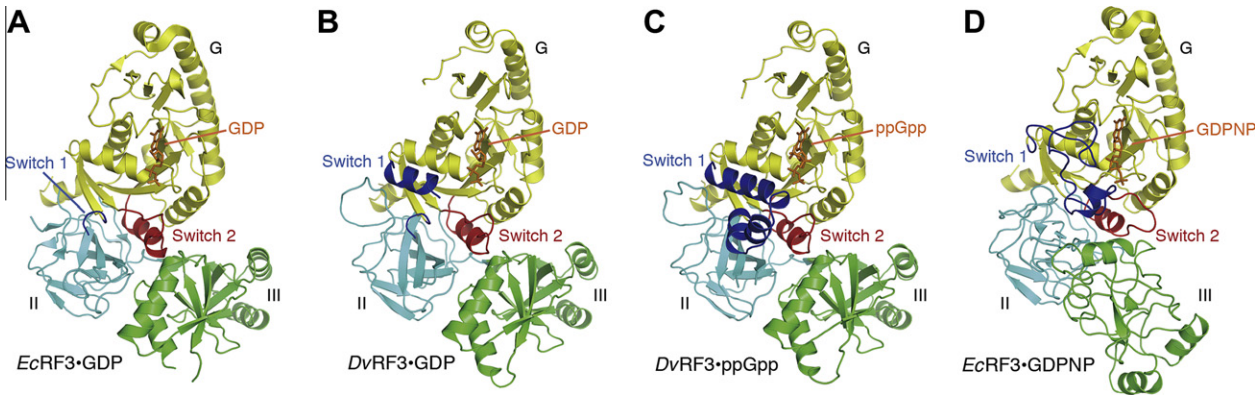

Fig. 1. Comparison of crystal structures of RF3. (A) *Ec*RF3•GDP (PDB code: 2h5e), (B) *Dv*RF3•GDP, (C) *Dv*RF3•ppGpp, (D) *Ec*RF3•GDPNP. G domain, Domain II and III are shown in yellow, cyan and green, respectively. Switch 1 and 2 regions are colored in blue and red, respectively. GDP, ppGpp and GDPNP are shown as an orange stick model.

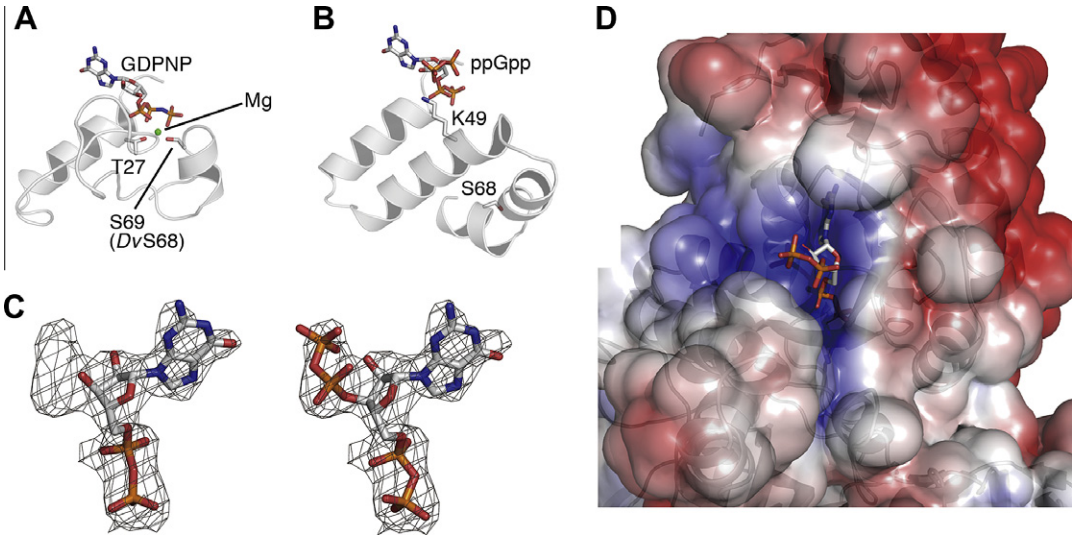

Fig. 2. The structures around the nucleotide-binding regions of RF3s. (A) ribosome-bound *Ec*RF3•GDPNP (PDB code: 3SFS). (B) *Dv*RF3•ppGpp (this study). Nucleotides are shown as stick models and Mg2+ as a green ball. (C) GDP and ppGpp are superimposed on the (*Fo-Fc*) map of *Dv*RF3 (Peak-2) contoured at 3σ. (D) The electrostatic potential mapped onto the solvent-accessible surface around the nucleotide binding region of *Dv*RF3•ppGpp. The positive and negative charges are shown in blue and red, respectively.

Table 1
The recycling efficiencies by RF3 variants and comparison between the ppGpp- and GDP-binding affinity of each variant.

	Recycling efficiency* (%)	Affinity index**
−RF3	89	–
DvRF3	32	2
Dv K49G	46	0.1
Dv A47G	68	1–2
EcRF3	50	0.1
Ec G50K	46	0.2
Ec G48A G50K	56	0.2–0.5

* "The recycling efficiency" means activity rate in the presence of ppGpp compared with the absence of ppGpp.
** "Affinity index" means the ratio of [GDP]/[ppGpp] when GDP- and ppGpp-bound forms are present in equal amounts.

A47G of *Dv*RF3, and G50K and G48A/G50K of *Ec*RF3 were examined by a gel-shift assay (Fig. S4, Table 1). Since the concentration of GDP is at most 0.2 mM (Table S3) in prokaryotes, 0.2 mM of GDP was added to all samples except for the control in the following experiments. When the ppGpp concentration was equal to GDP (0.2 mM), wild-type protein predominantly existed as *Dv*RF3•ppGpp: in 1 mM ppGpp, it was mostly present as *Dv*RF3•ppGpp. In the case of *Dv*RF3-K49G, however, only half of the molecules were in the ppGpp-bound form in 2 mM ppGpp. The binding affinity rate of ppGpp/GDP for *Dv*RF3-K49G was approximately 20-fold lower than that of the wild-type protein (approximately equal to that of wild-type *Ec*RF3), whereas that of *Dv*RF3-A47G was not significantly reduced. These results suggest that the Lys49 of *Dv*RF3 contributes to the high selectivity for ppGpp rather than GDP (Fig. S4). In case of *Ec*RF3, the G50K mutant did not exhibit a distinct increase in affinity for ppGpp, but G48A/G50K showed an increased affinity rate of ppGpp/GDP, even though this was clearly lower than that of wild-type *Dv*RF3. When *E. coli* strain BL21 (DE3) cells transformed with plasmids encoding each RF3 variant was grown in M9-casamino acids medium and harvested after exponential phase of growth, however, all of the RF3 variants described above were revealed to be in the ppGpp-bound form (Fig. 4A). These results suggest that the intracellular level of ppGpp under conditions that induce the stringent response is sufficient to produce the ppGpp-bound form as the major fraction of RF3 molecules (Table S3).

3.4. RF1 recycling assay

In the absence of RF3, the efficiency of RF1 recycling was not affected by the presence or the absence of ppGpp (Fig. 4B and Table 1). On the contrary, recycling was 3.3- and 2.4-fold accelerated by wild-type *Ec*RF3 and *Dv*RF3, respectively, in the absence of ppGpp, whereas they were strongly reduced in the presence of ppGpp. It should be noted that deceleration of recycling by *Dv*RF3 in the presence of ppGpp was more pronounced than the deceleration by *Ec*RF3. The RF1 recycling activities of both *Dv*RF3 and *Ec*RF3 in the absence of ppGpp were slightly altered by the introduction of mutations in the switch-1 region. On the contrary, the recycling activities were significantly reduced in the presence of ppGpp for all mutants except for *Dv*RF3-A47G. Though these simple mutation experiments at corresponding region did not explain the inhibition efficiency by the specific residues, it is clear that ppGpp inhibits RF3 activity because the inhibition efficiency was not correlated with the affinity rate of ppGpp/GDP in this experiment (Fig. 4 and Table 1). Taken together, GDP accelerates the recycling of RF1 under nutrient-rich growth conditions, whereas ppGpp may decelerate the recycling under stringent conditions.

According to this hypothesis, the binding of ppGpp to RF3 may affect the interaction between RF3 and the ribosome. To investigate possible effects on the interaction between ppGpp in RF3 and the sarcin–ricin loop (SRL) region, a model for ribosome•*Dv*RF3•ppGpp complex was generated by superposing *Dv*RF3•ppGpp on the structure of an *Ec*RF3-bound ribosome in the GDPNP form (PDB code 3SFS). In this model, three domains of *Dv*RF3 were independently fitted into *Ec*RF3•GDPNP (Fig. 3A and B). In the structure of ribosome•*Ec*RF3•GDPNP, A2662 of SRL, which is important for the activation of translational GTPases by ribosome does not form a contact with GDPNP or RF3 [12], but G2663 and G2664 interact with Lys47 and Arg49 (Fig. 3A). In the model of ribosome•*Dv*RF3•ppGpp, the 3′ diphosphate group of ppGpp protrudes from the molecular surface of RF3, and makes a clash and electrostatic repulsion with the phosphate group of A2662 in the SRL, suggesting that it interferes with the plausible direct interaction of RF3 with the SRL (Fig. 3B).

The reduction of RF3-dependent RF1 recycling on the release complex in the presence of ppGpp may be insignificant for a single

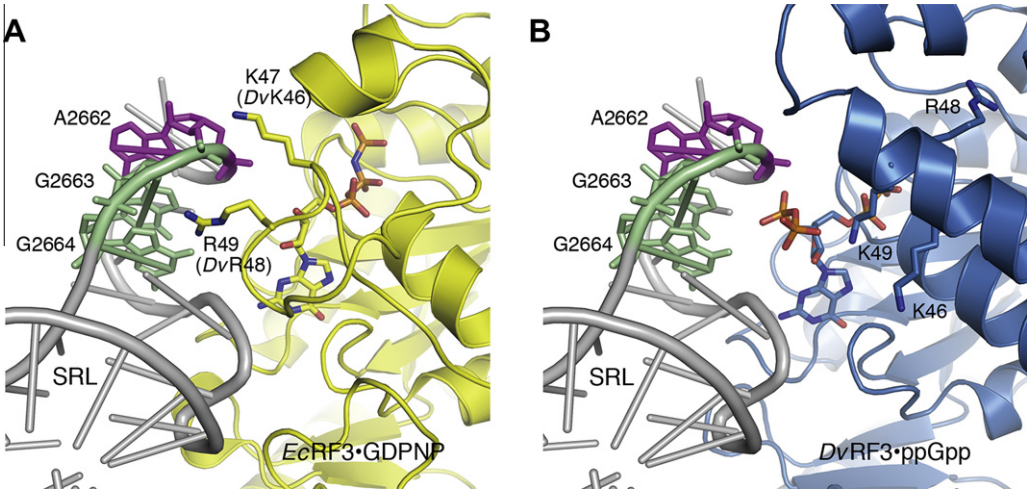

Fig. 3. Interactions of RF3 with the 70S Ribosome. (A) Structure of ribosome•*Ec*RF3•GDPNP. (B) A model of ribosome•*Dv*RF3•ppGpp superimposed on the structure of ribosome•*Ec*RF3•GDPNP by a rigid-body docking simulation. SRL main-chain, G2663-G2664 and A2662 are colored in gray, green and magenta, respectively. *Ec*RF3 and *Dv*RF3 are shown as yellow and dark-blue ribbon models, respectively. GDPNP, ppGpp, K47, R49 (*Ec*RF3) and K49 (*Dv*RF3) are shown as a stick model. Nitrogen, oxygen and phosphate atoms are colored in blue, red and orange, respectively.

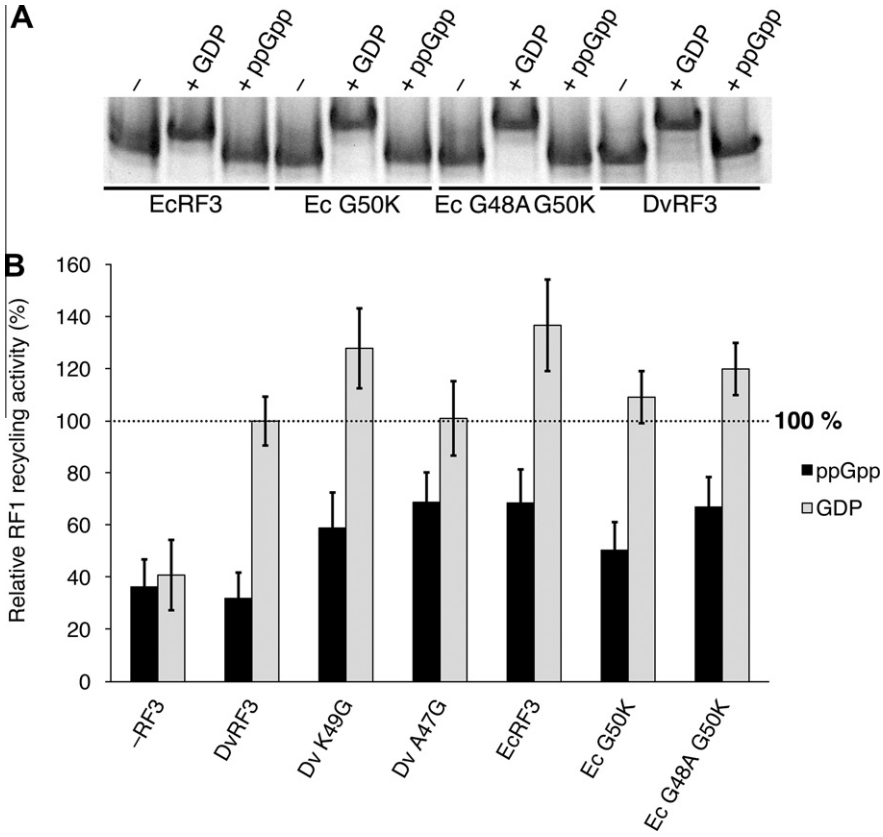

Fig. 4. Gel-shift and RF1 recycling assays of RF3 variants. (A) RF3 proteins prepared from the cells harvested after exponential phase of growth were separated by native PAGE. "+GDP" and "+ppGpp" were pre-incubated with 1 mM of GDP and ppGpp, respectively. (B) RF1 recycling assay in the presence (black) or the absence (gray) of ppGpp were assayed in vitro. Recycling activity with RF3 in the absence of ppGpp was taken as 100%. Error bars represent standard deviation of four replicates.

release complex (Fig. 4B and Table 1). However, repression of the RF1 recycling by RF3•ppGpp must affect overall ribosome traffic, and a total amount of the translational products could be significantly reduced, since polysomes are formed in the bacterial cells [13]. It is known that a decrease in the translation rate at one codon causes a crowd of downstream ribosome like a traffic jam on a highway, resulting in a serious decline in the whole translation rate. These lines of evidence suggest that RF3 functions as a cellular metabolic sensor and regulator that switches between the active GDP-bound form and the inactive ppGpp-bound form.

There may be another way to understand the role of ppGpp in bacteria. As noted above, most bacteria have either glycine or lysine at position 49. The glycine group is mainly composed of enterobacteria, whereas deltaproteobacteria, such as *Desulfovibrio* species, have a lysine residue (Table S4), suggesting that deltaproteobacteria require a lysine residue and strict controls of transla-

tion rate in order to adapt to the environmental changes such as the stress of nutritional shortage. In addition, there is another possibility, namely, that bacteria that do not exhibit a large variation in their intracellular ppGpp concentration (e.g. *Desulfovibrio* sp.) are sensitive to ppGpp. According to this hypothesis, ppGpp is not a special ligand for the stringent response, but a simple "switching" factor that allows bacteria to respond appropriately to the changes of nutritional condition in deltaproteobacteria.

Since translational Gtpases except RF3 enter into ribosome as a GTP-bound form, but RF3 as a GDP-bound form, it is conceivable that RF3 as ppGpp-bound form has a direct influence on translation in ribosome. However, it is also reported that IF2 in the GDP-bound form binds to ribosome and IF2•ppGpp has an influence on initiation step. It is presumed that EF-G and EF-Tu have the same possibility as IF2 [14].

4. PDB accession number

Coordinates and structure factors of *Dv*RF3•GDP and *Dv*RF3•ppGpp have been deposited in the Protein Data Bank (accession number 3VQT, 3VR1).

Acknowledgements

We are grateful to Dr. N. Shimizu, Dr. M. Kawamoto and Dr. M. Yamamoto at SPring-8 for their help during data collection at synchrotron beamline BL41XU. This work was supported in part by Grants-in-Aid from the GCOE Programs (YH) and for Scientific Research from MEXT (18GS0207) (YH), 22370061 (YH), and 22657031 (YH), the Japanese Aerospace Exploration Agency Project (YH). We also thank the NBRP (NIG, Japan): *E. coli* for providing the ASKA clone (−) JW5873 used in this work.

Appendix A. Supplementary data

Supplementary data associated with this article can be found, in the online version, at http://dx.doi.org/10.1016/j.febslet.2012.08.029.

References

[1] Freistroffer, D.V., Pavlov, M.Y., MacDougall, J., Buckingham, R.H. and Ehrenberg, M. (1997) Release factor RF3 in *E. coli* accelerates the dissociation of release factors RF1 and RF2 from the ribosome in a GTP-dependent manner. EMBO J 16, 4126–4133.
[2] Zhou, J., Lancaster, L., Trakhanov, S. and Noller, H.F. (2012) Crystal structure of release factor RF3 trapped in the GTP state on a rotated conformation of the ribosome. RNA 18, 230–240.
[3] Gao, H. et al. (2007) RF3 induces ribosomal conformational changes responsible for dissociation of class I release factors. Cell 129, 929–941.
[4] Jin, H., Kelley, A.C. and Ramakrishnan, V. (2011) Crystal structure of the hybrid state of ribosome in complex with the guanosine triphosphatase release factor 3. Proc. Natl. Acad. Sci. USA 108, 15798–15803.
[5] Wittinghofer, A. and Vetter, I.R. (2011) Structure-function relationships of the G domain, a canonical switch motif. Annu. Rev. Biochem. 80, 943–971.
[6] Buckstein, M.H., He, J. and Rubin, H. (2008) Characterization of nucleotide pools as a function of physiological state in *Escherichia coli*. J. Bacteriol. 190, 718–726.
[7] van der Biezen, E.A., Sun, J., Coleman, M.J., Bibb, M.J. and Jones, J.D. (2000) Arabidopsis RelA/SpoT homologs implicate (p)ppGpp in plant signaling. Proc. Natl. Acad. Sci. USA 97, 3747–3752.
[8] Kihira, K. et al. (2008) Crystallization and preliminary X-ray analysis of a class II release factor RF3 from a sulfate-reducing bacterium. Acta Crystallogr. Sect. F: Struct. Biol. Cryst. Commun. 64, 622–624.
[9] Shimizu, Y., Inoue, A., Tomari, Y., Suzuki, T., Yokogawa, T., Nishikawa, K. and Ueda, T. (2001) Cell-free translation reconstituted with purified components. Nat. Biotechnol. 19, 751–755.
[10] O'Neil, K.T. and DeGrado, W.F. (1990) A thermodynamic scale for the helix-forming tendencies of the commonly occurring amino acids. Science 250, 646–651.
[11] Lyu, P.C., Liff, M.I., Marky, L.A. and Kallenbach, N.R. (1990) Side chain contributions to the stability of alpha-helical structure in peptides. Science 250, 669–673.
[12] Voorhees, R.M., Schmeing, T.M., Kelley, A.C. and Ramakrishnan, V. (2010) The mechanism for activation of GTP hydrolysis on the ribosome. Science 330, 835–838.
[13] Mitarai, N., Sneppen, K. and Pedersen, S. (2008) Ribosome collisions and translation efficiency: optimization by codon usage and mRNA destabilization. J. Mol. Biol. 382, 236–245.
[14] Milon, P. et al. (2006) The nucleotide-binding site of bacterial translation initiation factor 2 (IF2) as a metabolic sensor. Proc. Natl. Acad. Sci. USA 103, 13962–13967.